Optimal configurations for normal-metal traps in transmon qubits

A. Hosseinkhani,[1,2] R.-P. Riwar,[1,3] R. J. Schoelkopf,[3] L. I. Glazman,[3] and G. Catelani[1]

[1]*JARA-Institute for Quantum Information (PGI-11),*
Forschungszentrum Jülich, 52425 Jülich, Germany
[2]*JARA-Institute for Quantum Information, RWTH Aachen University, D-52056 Aachen, Germany*
[3]*Departments of Physics and Applied Physics, Yale University, New Haven, CT 06520, USA*
(Dated: November 25, 2017)

Controlling quasiparticle dynamics can improve the performance of superconducting devices. For example, it has been demonstrated effective in increasing lifetime and stability of superconducting qubits. Here we study how to optimize the placement of normal-metal traps in transmon-type qubits. When the trap size increases beyond a certain characteristic length, the details of the geometry and trap position, and even the number of traps, become important. We discuss for some experimentally relevant examples how to shorten the decay time of the excess quasiparticle density. Moreover, we show that a trap in the vicinity of a Josephson junction can significantly reduce the steady-state quasiparticle density near that junction, thus suppressing the quasiparticle-induced relaxation rate of the qubit. Such a trap also reduces the impact of fluctuations in the generation rate of quasiparticles, rendering the qubit more stable.

I. INTRODUCTION

For a successful execution of quantum gates, the participating qubits must have coherence times exceeding the gate operation time. Moreover, the longer the coherence time, the less resources are needed for the implementation of error correction. Thus, it is important to understand and control decoherence mechanisms. Over the past several years it has been firmly established, both theoretically [1–3] and experimentally [4–8], that quasiparticles are detrimental to superconducting qubits based on Josephson junctions. For example, tunneling of quasiparticles through a transmon junction leads to a relaxation rate proportional to their density. At the low temperatures the qubits are operated, the number of quasiparticles in typical devices should be negligible in thermal equilibrium; however, the measured quasiparticle density is several orders of magnitude larger than expected, indicating that quasiparticle generation mechanisms of unknown origin are maintaining a large non-equilibrium quasiparticle population. While in general it is not possible to control the poorly understood generation processes, trapping quasiparticles away from the junctions offers a way to limit their unwanted effects. In this paper we build on a recently developed model [9] for trapping by normal-metal islands to explore ways to optimize the traps performance.

A number of approaches to trap quasiparticles have been explored, from gap engineering [10, 11] to trapping by vortices [12–15] and normal-metal islands [16–19]. In all cases, trapping is made possible by energy relaxation of excitations inside the trap, since an excitation with energy below the gap Δ of the device's superconductor S cannot return to S. For normal-metal traps in tunnel contact with S, the interplay between tunneling and relaxation was studied both theoretically and experimentally in Ref. [9], with the measurements indicating that relaxation is the bottleneck limiting the trapping rate. The considerations in Ref. [9] were mostly limited to the decay dynamics of excess quasiparticles in a model of a point-like trap placed in a (quasi-)one-dimensional wire; in contrast, here we examine finite-size traps in realistic qubit geometries. We focus on a qubit design, the coplanar gap capacitor transmon of Ref. [14], whose coherence was shown to be limited by quasiparticles. Similarly, the relaxation time of a fluxonium biased close to (but not at) the half flux quantum [8] and that of a flux qubit [20] were found to be limited by quasiparticles. In other experiments with transmons (in a different design with large pads rather than gap capacitor plus small pads), quasiparticles were not the limiting factor, but there was evidence that they will become relevant if the coherence time is to be increased by another order of magnitude [7]. In addition to this kind of qubits, quasiparticles are detrimental to both the so-called Andreev level qubit [21, 22] and potentially to future devices based on Majorana states [23] – in both cases, coherence is destroyed by a single quasiparticle changing the parity of the state. Quasiparticles are also a source of errors in charge pumps comprising superconducting elements, which hampers their use in metrological applications – indeed, traps have been used to increase the pump accuracy [24]. Therefore, the analysis presented here for a particular case can potentially indicate the way for engineering better trap configurations in a variety of systems, since it is based on a phenomenological diffusion equation which is expected to hold quite generally.

In this paper we show that use of quasi-1D geometries facilitates trapping with small traps, and that their positions can be optimized. We consider three ways in which normal-metal traps may improve qubit performance. First, we note that events which generate a large number of quasiparticles render the qubit inoperable so long as the excess quasiparticles are not eliminated; here we find the parameters and placement of traps that enhance the relaxation rate of the excess density. Second, in addition to the dynamics of the excess density, we study the quasiparticles steady-state density in the presence of

a generic generation mechanism with a rate determined by experiments [14, 25]; we find that a trap placed near a junction can suppress the quasiparticle density at that junction, potentially leading to a longer T_1 relaxation time for the qubit. Third, we consider the effect of fluctuations in the generation rate: they lead to the fluctuation in the quasiparticle density near the junction and, associated with it, to variations of a qubit T_1 [20, 25]; placing a trap up to a certain distance from the junction can reduce the density fluctuations and hence make the qubit more stable.

The paper is organized as follows: in Sec. II we summarize the model of Ref. [9] to establish our notation and for the paper to be self-contained. In Sec. III we consider a realistic qubit geometry, namely the coplanar gap capacitor transmon of Refs. [9, 14]; we give analytical arguments for trap configurations leading to faster relaxation rates of the excess density – see Eq. (10) for the single trap case and Eqs. (18) and (19) for the multi-trap one – and complement those with numerical calculations whose outcomes are summarized in Figs. 2 to 4. In Sec. IV we turn our attention to the steady-state density at the junction and its fluctuations; both can be suppressed by appropriately placed traps, but while the steady-state density always increases monotonically with trap-junction distance [Eq. (25)], we find for a strong trap a non-monotonic behavior of fluctuations [Eq. (39)] and hence an optimal trap position. We summarize our findings in Sec. V. A number of Appendices complement the main text: in Appendix A we compare trapping by normal-metal traps with that due to vortices; in Appendix B we present some mathematical details for the case of a single, finite-size trap, and Appendix C addresses the question of the experimental observability of the slowest decay rate of the excess density; Appendices D and E contain details about the mapping of a realistic qubit design into a 1D wire; finally Appendix F considers traps in the Xmon qubit geometry.

II. THE EFFECTIVE TRAPPING RATE MODEL

Superconducting qubits are generically fabricated by depositing thin superconducting films over an insulating substrate; we therefore consider quasiparticles as diffusing in a two-dimensional region. Normal-metal (N) traps are also thin films deposited on top of the superconductor S, and we assume that an insulating barrier of low transparency is present between N and S. Then the dynamics of the (normalized) quasiparticle density in the superconductor x_{qp} is captured by a generalized diffusion equation

$$\dot{x}_{\mathrm{qp}} = D_{\mathrm{qp}} \vec{\nabla}^2 x_{\mathrm{qp}} - \mathcal{A}(\vec{x}) \Gamma_{\mathrm{eff}} x_{\mathrm{qp}} - s_{\mathrm{b}} x_{\mathrm{qp}} + g \quad (1)$$

(see Ref. [9] for theoretical justification and experimental validation of this effective model). The quasiparticle density x_{qp} is normalized by the Cooper pair density $\nu_0 \Delta$

and is therefore a dimensionless quantity; it is a function of time t (the dot denotes the time derivative) and position $\vec{x}$ in the x-y plane (here ν_0 is the density of states at the Fermi level). The phenomenological diffusion constant D_{qp} is proportional to the normal-state diffusion constant for electrons in the superconductor, D_S. The term proportional to the effective trapping rate Γ_{eff} accounts for trapping of quasiparticles by the normal metal and is discussed in more detail below. The function $\mathcal{A}(\vec{x})$ is unity when $\vec{x}$ is within the S-N contact region and zero otherwise – in other words, this function localizes the trap to only a part of the whole device, rendering the system inhomogeneous, whereas the other coefficients in Eq. (1) are constant throughout the superconductor. The rate g describes the generation of quasiparticles. Finally, the possibility that other mechanisms can trap quasiparticles in the bulk of the superconductor is captured by the term proportional to the background trapping rate s_{b}; we set $s_b = 0$ in this paper, as its effect is negligible [26].

The effective trapping rate Γ_{eff} incorporates the interplay between tunneling from S to N at rate Γ_{tr}, relaxation in N with rate Γ_{r}, and escape from N to S with rate Γ_{esc}. For a quasiparticle distribution at an (effective) temperature $T \ll \Delta$, we can distinguish two limiting cases. For fast relaxation, $\Gamma_{\mathrm{r}} \gg (\Delta/T)^{1/2} \Gamma_{\mathrm{esc}}$, the effective trapping rate is determined by the S to N tunneling rate, $\Gamma_{\mathrm{eff}} \approx \Gamma_{\mathrm{tr}}$: since quasiparticles loose energy quickly upon entering into N, they cannot tunnel back to S. For slow relaxation, $\Gamma_{\mathrm{r}} \ll (\Delta/T)^{1/2} \Gamma_{\mathrm{esc}}$, on the other hand, we have $\Gamma_{\mathrm{eff}} \approx (2T/\pi\Delta)^{1/2} \Gamma_{\mathrm{tr}} \Gamma_{\mathrm{r}}/\Gamma_{\mathrm{esc}}$; typically $\Gamma_{\mathrm{esc}} \approx \Gamma_{\mathrm{tr}}$, hence the effective rate is limited by the relaxation process and becomes temperature dependent. The experimental results from Ref. [9] indicate that the trapping is relaxation-limited; this implies that making the S-N contact more transparent would not affect the trapping rate Γ_{eff}. This holds for a contact in the tunneling regime, so that the proximity effect can be neglected; for good contact between S and N, the gap would be suppressed and the trapping would be more appropriately described as being due to gap engineering – this regime is outside the scope of the present work.

As discussed in the introduction, we are interested in three quantities which are affected by the trap: the relaxation rate of the excess density (i.e., the density which is in addition to the steady-state one), the steady-state density at the junction and its fluctuations. Focusing on the dynamics of the excess density, we note that the diffusion equation (1) can be solved in terms of eigenmodes, each with an eigenvalue corresponding to the decay rate of that mode. In general, at long times the slowest mode determines the exponential decay of the excess density, which therefore can be written as

$$x_{\mathrm{qp}}(t, \vec{x}) \simeq x_{\mathrm{qp}}^0(\vec{x}) e^{-t/\tau_w} , \quad (2)$$

where the decay rate τ_w^{-1} is the eigenvalue with the smallest absolute value, and x_{qp}^0 its corresponding eigenfunction. Simple estimates for τ_w can be found in limiting

A. Optimization for a single trap

Let us consider a single trap placed in the antenna wire of length L, see Fig. 1 (the device being symmetric, there are two traps in total). We start for simplicity with a short trap of length $d \ll \lambda_{\rm tr}$ and neglect the gap capacitor and antenna pads; we then show how to map the full device to this simpler configuration and compare our estimates with numerical results.

For a short trap in a wire, the diffusion equation (1) can be written in the form (cf. Appendix B)

$$\dot{x}_{\rm qp} = D_{\rm qp}\vec{\nabla}^2 x_{\rm qp} - \gamma_{\rm eff}\delta\left(y - L_1\right)x_{\rm qp}. \quad (7)$$

The trap is at position $y = L_1$ and $\gamma_{\rm eff} = d\Gamma_{\rm eff}$. Consider for simplicity the case $\gamma_{\rm eff} \to \infty$, such that quasiparticles are trapped immediately once they reach the trap. As a consequence, $x_{\rm qp}(L_1) = 0$, and the density on the left and right sides of the trap decays with the rates $\tau_w^{-1} = \pi^2 D_{\rm qp}/4L_1^2$ and $\tau_w^{-1} = \pi^2 D_{\rm qp}/4(L - L_1)^2$, respectively. If the trap is at the center of the wire, $L_1 = L/2$, the density decays equally fast on both sides, and the decay rate of the slowest mode is four times faster as compared to placing the trap at the beginning or end of the wire. In other words, the central position is the optimal one for the trap to evacuate quasiparticles as quickly as possible.

At finite $\gamma_{\rm eff}$, the left/right modes are coupled, but the coupling is small provided that the trap is strong, $d \gg l_0$. The coupling lifts the mode degeneracy at $L_1 = L/2$, but does not change the above conclusion on the optimal position. We note, however, that if quasiparticles are injected and detected locally (as, e.g., in Ref. [9]) one may not necessarily observe the global slowest decay rate for strong traps; see Appendix C for more details.

In the simple example above we have shown that the optimal trap position (for which the decay rate of the slowest mode is the fastest) is such that the diffusion times in both sides of the trap are equal. We can extend this finding to a more realistic qubit geometry [9] which includes the coplanar gap capacitor close to the Josephson junction and the antenna pad at the far end of the wire, see Fig. 1. The capacitor "wings" of length L_c and the square pad with side $L_{\rm pad}$ can be accounted for by adding some effective lengths to the antenna wire. The effective lengths $L_c^{\rm eff}(k)$ and $L_{\rm pad}^{\rm eff}(k)$ (for capacitor and pad, respectively) in general depend on the wave vector k, see Appendices D and E. If these effective lengths are much smaller than the wire length L, we find that for the slow modes the dependence on k drops out: $L_{\rm pad}^{\rm eff} \approx L_{\rm pad}^2/W$ and $L_c^{\rm eff} \approx 2\frac{W_c}{W}L_c$, with W and W_c the widths of the wire and capacitor wings, respectively. These effective lengths may simply be added to the lengths to the left and right of the trap to find the decay rates:

$$\frac{1}{\tau_w} = \frac{\pi^2 D_{\rm qp}}{4\left(L - L_1 + L_{\rm pad}^2/W - d/2\right)^2} \quad (8)$$

for the right mode and

$$\frac{1}{\tau_w} = \frac{\pi^2 D_{\rm qp}}{4\left(L_1 + 2\frac{W_c}{W}L_c - d/2\right)^2} \quad (9)$$

for the left mode; we have accounted for the finite size of the trap by subtracting the $d/2$ terms in the denominators, and L_1 denotes the trap center. Thus, the optimal trap position is (in the strong trap limit):

$$L_{\rm opt} = \frac{L}{2} + \frac{L_{\rm pad}^{\rm eff} - L_c^{\rm eff}}{2}. \quad (10)$$

The optimal position is closer to the pad (gap capacitor) if the effective length of the pad (capacitor) is larger.

We can check the validity of the above considerations for strong traps and extend our consideration to weaker (i.e., smaller) traps by more accurately modelling the diffusion in the device as done in the Supplementary Information of Ref. [14] (see also Appendix A). Namely, the density in the parts not covered by the trap is written in the form

$$x_{\rm qp}(t, y) = e^{-t/\tau_w}\left[\alpha\cos ky + \beta\sin ky\right] \quad (11)$$

with $1/\tau_w = D_{\rm qp}k^2$ (except for the pad, where the density is assumed uniform), while under the trap we have

$$x_{\rm qp}(t, y) = e^{-t/\tau_w}\left[\alpha\cosh y/\lambda + \beta\sinh y/\lambda\right]. \quad (12)$$

Imposing continuity of $x_{\rm qp}$ and current conservation we find:

$$z^2 + b^2 = \left(L/\lambda_{\rm tr}\right)^2, \quad (13)$$

$$\frac{z}{b}\left[az + \tan\left(z\xi_R\right)\right]\left[1 - h\left(z, \xi_L\right)\tanh\left(b\frac{d}{L}\right)\right]$$
$$-\left[1 - az\tan\left(z\xi_R\right)\right]\left[\tanh\left(b\frac{d}{L}\right) - h\left(z, \xi_L\right)\right] = 0, \quad (14)$$

with $z = kL$, $b = L/\lambda$, $a = L_{\rm pad}^2/(LW)$, and

$$h\left(z, \xi_L\right) = \frac{z}{b}\frac{\tan\left(z\xi_L\right) + \tan\left(z\frac{l}{L}\right) + 2\frac{W_c}{W}\tan\left(z\frac{L_c}{L}\right)}{1 - \tan\left(z\xi_L\right)\left[\tan\left(z\frac{l}{L}\right) + 2\frac{W_c}{W}\tan\left(z\frac{L_c}{L}\right)\right]}. \quad (15)$$

We also define the (normalized) length of the wire to the left (right) of the trap by

$$\xi_L = \left(L_1 - d/2\right)/L, \quad (16)$$
$$\xi_R = \left(L - L_1 - d/2\right)/L. \quad (17)$$

Solving Eqs. (13) and (14) for z and b, one can find the density decay rate $1/\tau_w = D_{\rm qp}z^2/L^2$. For a long qubit with $L \gg \lambda_{\rm tr}$, we find for the slow modes $b \approx L/\lambda_{\rm tr} \gg 1$ and $z \sim 1$. We note that the assumption of uniform density in the pad requires $1/\tau_w = D_{\rm qp}z^2/L^2 \ll D_{\rm qp}/L_{\rm pad}^2$; since for experimentally relevant parameters we have $L_{\rm pad}^2/L^2 \sim 10^{-2}$, the assumption is valid for slow modes even when $z \gtrsim 1$.
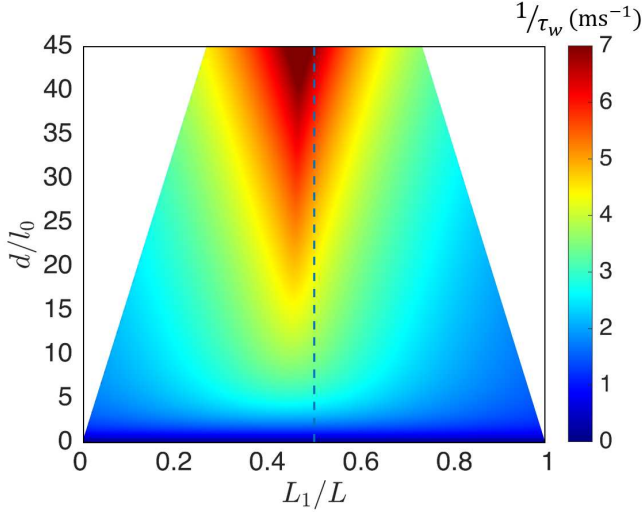
FIG. 2. Trapping rate $1/\tau_w$ as a function of the trap position L_1 (in units of L) and normalized trap size d/l_0 – see Fig. 1 for the device geometry; the device parameters are: $L = 1\,\text{mm}$, $l = 60\,\mu\text{m}$, $W = 12\,\mu\text{m}$, $L_c = 200\,\mu\text{m}$, $W_c = 20\,\mu\text{m}$, $L_{\text{pad}} = 80\,\mu\text{m}$. We used $\lambda_{\text{tr}} = 86.2\,\mu\text{m}$ for the trapping length, so $l_0 = \pi\lambda_{\text{tr}}^2/2L \simeq 11.7\,\mu\text{m}$. The white areas are regions in which the trap center cannot be pushed closer to or further away from the gap capacitor due to the finite trap size.

In Fig. 2 we show a density plot of the decay rate $1/\tau_w$ as a function of the distance L_1 between gap capacitor and trap center and of the normalized trap size d/l_0, calculated using typical experimental parameters as detailed in the caption. For a strong trap, $d \gg l_0$, as discussed in Sec. II we find that the decay rate is sensitive to the trap position. The optimum position is shifted with respect to the middle of the wire (dash-dotted line in Fig. 2), in agreement with the prediction of Eq. (10). Indeed, for the parameters in Fig. 2, we find $L_{\text{pad}}^{\text{eff}} = L_{\text{pad}}^2/W \approx 533\,\mu\text{m}$ and $L_c^{\text{eff}} = 2\frac{W_c}{W}L_c \approx 667\,\mu\text{m}$, and the optimal position is closer to the gap capacitor.

When the trap size is $d \lesssim l_0$, the trap position has only a minor effect on the trapping rate. This is more clearly seen in Fig. 3 (bottom solid curve). For longer traps, we compare the decay from the numerical solution to Eqs. (13) and (14) with Eqs. (8) and (9). When the trap is strong but still short compared to the wire (middle solid), Eqs. (8) and (9) (dashed) provide a good approximation to the numerical results (in fact, one can expect the numerically calculated rate to be slower than the analytical prediction, since the numerics account for the finite trapping length which allows for finite density under the trap as well as for the bridge of length l joining the junction to the gap capacitor). For very long traps (upper solid line) the approximation that the effective lengths are small compared to the (uncovered part of the) wire fails, and the calculated rate is faster; this is qualitatively in agreement with the fact that as the mode wavelength increases, the effective lengths decrease, see
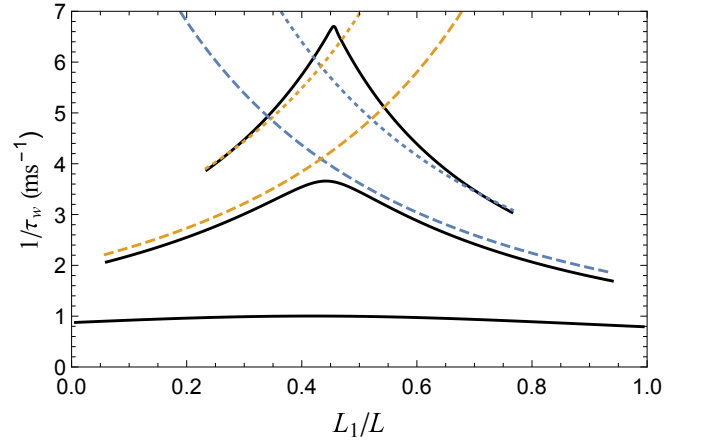
FIG. 3. Solid lines: trapping rate $1/\tau_w$ as a function of the trap position L_1 measured in units of L for (top to bottom) $d/l_0 = 40, 10, 1$; other parameters are specified in the caption to Fig. 2 and the device geometry is shown in Fig. 1. The dashed lines are the estimates provided by Eqs. (8) and (9) for $d/l_0 = 40, 10$.

Eqs. (D4) and (E2) (for the gap capacitor, this is true so long as $2W_c/W > 1$).

Our focus so far has been in speeding up the decay rate of the slowest mode, without taking into consideration the amplitude of the mode at the junction. This approach is correct for weak traps, $d \lesssim l_0$, since the amplitude of the mode is approximately the same on both sides of the trap. For strong but small traps, $l_0 \ll d \lesssim \lambda_{tr}$, the amplitude on one side of the trap is algebraically suppressed by a factor of order d/l_0 compared to the amplitude on the other side (see Appendix C), while for long traps, $d \gg \lambda_{\text{tr}}$ the suppression is exponential in d/λ_{tr} (see Appendix B). In the latter case, it would clearly be advantageous to place the trap close to the junction: the mode with large amplitude between junction and trap would decay quickly, while the slow mode with large amplitude on the other side of the trap would decay slowly but it would be exponentially suppressed at the junction. However, as pointed out at the end of Sec. II, long traps could be too lossy – this motivates us to further study how to obtain the fastest possible decay using only small traps.

B. Multiple traps

We now generalize the considerations of the previous section to the case of multiple traps (in each half of the qubit). For a weak trap, the effective trapping rate is proportional to the trap size [Eq. (3)] but independent of position; therefore, no change in the density decay rate can be expected by dividing a weak trap into smaller ones, since the total size is unchanged. The strong-trap regime is qualitatively different in this regard. Let us consider N_{tr} strong traps in a wire of length L; the traps

separate the wire into $N_{tr}+1$ compartments. The optimal trap placement is obtained when the diffusion time is the same for each compartment, meaning that the traps have to be placed at positions $L_n = (2n-1)L/2N_{tr}$ with $n = 1, \ldots, N_{tr}$, and the resulting decay rate is

$$\tau_w^{-1}(N_{tr}) = N_{tr}^2 D_{qp} \frac{\pi^2}{L^2} \,. \tag{18}$$

The rate increases quadratically with the number of traps, so splitting a single strong trap into smaller pieces can highly increase the decay rate. However, when keeping the total area of the traps constant, there is a limitation to this improvement. Indeed, the length of each trap decreases as d/N_{tr} and the "device length" of each compartment is of order $L/2N_{tr}$; using these quantities in Eq. (5) we find that the traps cross over to the weak regime for

$$N_{tr}^{opt} \sim \sqrt{\frac{d}{2l_0}} \,; \tag{19}$$

here l_0 is defined by the right hand side of Eq. (5) with $L_{dev} = L$. Increasing the trap number beyond N_{tr}^{opt} does not further improve the decay rate, which is thus limited by Eq. (3). In other words, to obtain that maximum decay rate for given total length d, at least N_{tr}^{opt} traps should be placed evenly spaced over the device. Such a configuration could also reduce the trap-induced losses, since they depend on the trap position and size [27].

Let us now show in a concrete example that multiple traps can indeed increase the decay rate as predicted by Eq. (18). We consider again the transmon device depicted in Fig. 1, but we now assume that two traps are placed on the central wire, with distances L_1 and L_2 between the gap capacitor and the traps centers. Accounting for the second trap, we generalize Eq. (14) to

$$\frac{z}{b} \left[1 - h(z, \xi_L) \tanh \left(b\frac{d_1}{L} \right) \right] \left\{ \frac{z}{b} \tan(z\chi) - \tanh \left(b\frac{d_2}{L} \right) \right.$$
$$+ g(z, \xi_R) \left[1 - \frac{z}{b} \tan(z\chi) \tanh \left(b\frac{d_2}{L} \right) \right] \right\}$$
$$- \left[\tanh \left(b\frac{d_1}{L} \right) - h(z, \xi_L) \right] \left\{ \tanh \left(b\frac{d_2}{L} \right) \tan(z\chi) \right.$$
$$+ \frac{z}{b} - g(z, \xi_R) \left[\tan(z\chi) + \frac{z}{b} \tanh \left(b\frac{d_2}{L} \right) \right] \right\} = 0$$
$$\tag{20}$$

where, taking $L_1 < L_2$,

$$\xi_L = (L_1 - d_1/2)/L \,, \tag{21}$$
$$\xi_R = (L - L_2 - d_2/2)/L \,, \tag{22}$$
$$\chi = (L_2 - d_2/2 - L_1 - d_1/2)/L \,, \tag{23}$$

the function $h(z, \xi_L)$ is defined in Eq. (15), and

$$g(z, \xi_R) = \frac{z}{b} \frac{az + \tan(z\xi_R)}{1 - az \tan(z\xi_R)} \,. \tag{24}$$

We consider for simplicity the case of equal traps, $d_1 = d_2 \equiv d/2$ with $d = 20l_0 \simeq 233\,\mu m$ the total length of the normal metal. We show in Fig. 4 the decay rate as function of L_1 and L_2 for the same parameters as in Fig. 2. We find that the decay rate of the slowest mode is highest when placing the traps far away from each other, one trap touching the gap capacitor and the other begin close to the pad. This is in qualitative agreement with our expectations: consider again the gap capacitor and the pad as extra lengths added to the left and right of the central wire, respectively; this leads to a wire of effective total length $L_{tot} = L_c^{eff} + L + L_{pad}^{eff} \simeq 2200\,\mu m$. In such a wire the optimal positions would be $L_1 = L_{tot}/4 \simeq 550\,\mu m$ and $L_2 = 3L_{tot}/4 \simeq 1650\,\mu m$. The value of L_1 would indicate an optimal position inside the gap capacitor, but since we allow for the traps to be placed in the central wire only, this optimal placement is not possible. The value of L_2 corresponds to a position slightly away from the pad, in agreement with the results in Fig. 4. Finally, going from the optimally-placed single trap to the optimal two-trap configuration, the decay rate increases by a factor of ~ 3.4. This factor does not reach the theoretical maximum of 4 predicted by Eq. (18); the discrepancy can be attributed both to the non-optimal placement of the first trap mentioned above as well as to finite-size effects, as in the single trap case. However, the calculated improvement confirms that the decay rate can be significantly increased by optimizing the trap number and position.

It is instructive to compare our results for the two-trap case with the fast decay of the mode to the left of the single trap; using Eq. (9), we estimate the decay rate of this mode to be $1/\tau_w \simeq 14.7\,ms^{-1}$, slightly slower than the maximum rate shown in Fig. 4. In both cases, we do not allow the trap to enter the gap capacitor; this constraint could be important in limiting trap-related losses, as the gap capacitor is the region with the highest electric field. Using two traps we place only half the total normal material near the high-field region, while obtaining a slightly faster decay than with a single, large trap. For the considered example, further increase in the decay rate could be obtained by further splitting the traps. Indeed, a more accurate estimate for the length l_0 can be obtained by using $L_{dev} = L_{tot} - d \simeq 1967\,\mu m$ in Eq. (5), giving $l_0 \approx 5.9\,\mu m$. Then the "optimal" trap number would be $N_{tr}^{opt} \simeq \sqrt{d/2l_0} \sim 4$, requiring one trap to be placed on the pad, two on the antenna wire, and one on the gap capacitor (this placement is calculated using the "effective wire" length of the gap capacitor, so that in practice one should symmetrically place one trap on each of the two "wings" of gap capacitor). As mentioned above, placement on the gap capacitor could be detrimental, but with the optimal trap number only one quarter of the normal metal would be in the gap capacitor and the resulting losses would therefore be smaller than those due to a single large trap on the gap capacitor. Therefore, it is potentially beneficial to have multiple smaller traps in comparison with a single large trap. Such considerations
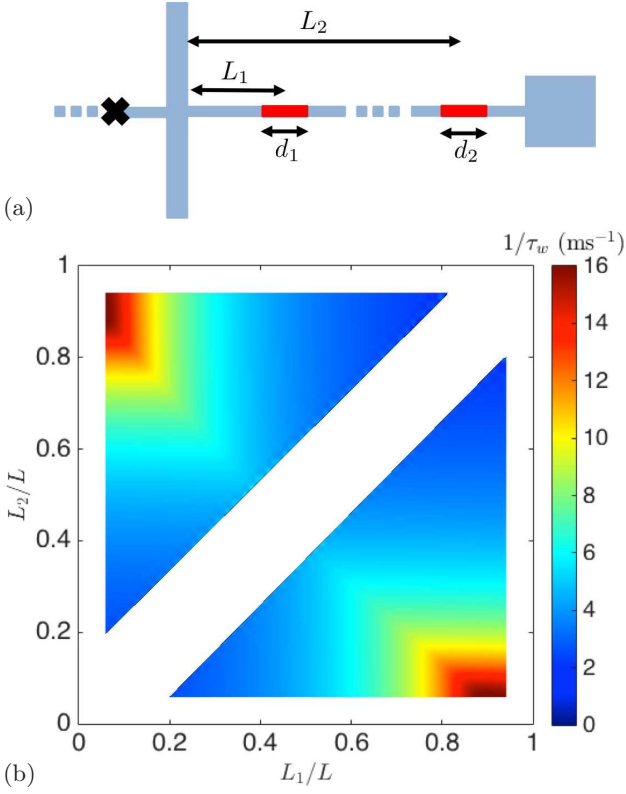
FIG. 4. (a) Device with two traps (dark red) in each half of the qubit; distances L_1 and L_2 are measured from the gap capacitor to the center of each trap, cf. Fig. 1. (b) Trapping rate $1/\tau_w$ as function L_1 and L_2; here the two traps are identical, $d_1 = d_2 = 10l_0$, which makes the plot symmetric under the exchange $L_1 \leftrightarrow L_2$. The parameters used are specified in the caption to Fig. 2. Similar to that figure, the white areas correspond to forbidden regions due to the finite traps' sizes . A comparison with Fig. 2 reveals that splitting a trap with length $d = 20l_0$ into two identical ones can boost the trapping rate up to a factor larger than 3.

are also dependent on the device design. In Appendix F we briefly consider a different geometry for the qubit, the Xmon of Ref. 29; the central X-shaped part of the device is small, and unfortunately this implies that no large gain in the decay rate can be obtained using multiple traps, so alternative approaches are desirable in this case. In the next section we turn our attention to the effect of traps on the steady-state density.

IV. SUPPRESSION OF STEADY-STATE DENSITY AND ITS FLUCTUATIONS

In the preceding section we have dealt with the question of how fast quasiparticles reach their steady state if there is a deviation from said steady-state density. In this section we point out that traps also affect the shape of the steady-state density. In particular, our aims are to minimize the steady-state density at the junction, which directly affects the T_1 time of qubits, as well as to stabilize

the density value against fluctuations in their generation rate which lead to temporal variations in the qubit lifetime. In our model, the steady-state density is nonzero due to a finite generation rate g in Eq. (1). As argued in Sec. II, in the presence of a weak trap the quasiparticle density is uniform, and in the steady-state takes the value $x_{qp}^s = g\tau_w$ with τ_w of Eq. (3). As we now show, going beyond the weak limit the geometry affects the spatial profile of the density.

For a concrete example, we consider the same geometry as in Sec. III A – that is, a single trap on the wire connecting gap capacitor and pad, see Fig. 1. The solution for the profile of the steady-state density in each 1D segment outside the trap is given by parabolas of the general form $x_{qp}^s = -y^2 g/2D_{qp} + \alpha y + \beta$, while under the trap we have $x_{qp}^s = \tilde{\alpha}\cosh(y/\lambda_{tr}) + \tilde{\beta}\sinh(y/\lambda_{tr}) + g/\Gamma_{eff}$. The pad density is again assumed constant. The parameters α, β in each segment, as well as $\tilde{\alpha}$, $\tilde{\beta}$ are found by imposing appropriate boundary conditions (i.e., continuity and current conservation). We finally arrive at the following expression for the steady-state density x_{qp}^J at the junction:

$$x_{qp}^J = \frac{g}{\Gamma_{eff}}\left[1 + \frac{1}{\sinh(d/\lambda_{tr})}\frac{A_R}{W\lambda_{tr}} + \coth(d/\lambda_{tr})\frac{A_L}{W\lambda_{tr}}\right] + \frac{g}{D_{qp}}\left[\frac{(L_1+l-d/2)^2}{2} + \frac{A_c(L_1-d/2)}{W}\right],$$
(25)

where $A_R = W[L - L_1 - d/2] + L_{pad}^2$ and $A_L = W[L_1 + l - d/2] + A_c$ are the uncovered areas to the right and left of the trap, respectively, and $A_c = 2W_cL_c$ is the gap capacitor area.

In the small trap limit, $d \ll \lambda_{tr}$, we can rewrite Eq. (25) in the form

$$x_{qp}^J \simeq g(\tau_w + t_D)$$
(26)

with τ_w defined in Eq. (3), while $t_D = [(L_1+l-d/2)^2/2 + A_c(L_1-d/2)/W]/D_{qp}$ represents the diffusion time between junction and trap (with the second term in square brackets taking into account the presence of the gap capacitor). Similar to the discussion in Sec. II, we can distinguish between an effectively weak ($\tau_w \gg t_D$) and strong trap ($\tau_w \ll t_D$), with the trap becoming strong as its length d increases above the position-dependent length scale $l_1 \sim \lambda_{tr}^2/\sqrt{D_{qp}t_D}$. Note that l_1 decreases with the distance L_1 between gap capacitor and trap and is always larger than l_0 of Eq. (5); therefore a trap that is weak in the sense of d being smaller than l_0 is weak at any position L_1, and the value of x_{qp}^J is only weakly dependent on the trap placement. On the other hand, a strong trap with $d > l_0$ effectively becomes weak, as L_1 decreases, when $\tau_w = t_D$. At positions L_1 smaller than that given by this condition, x_{qp}^J again becomes weakly dependent on trap placement. In other words, the condition determines the maximal distance at which the largest (up to numerical factor) suppression of x_{qp}^J is achieved for a given trap size d.
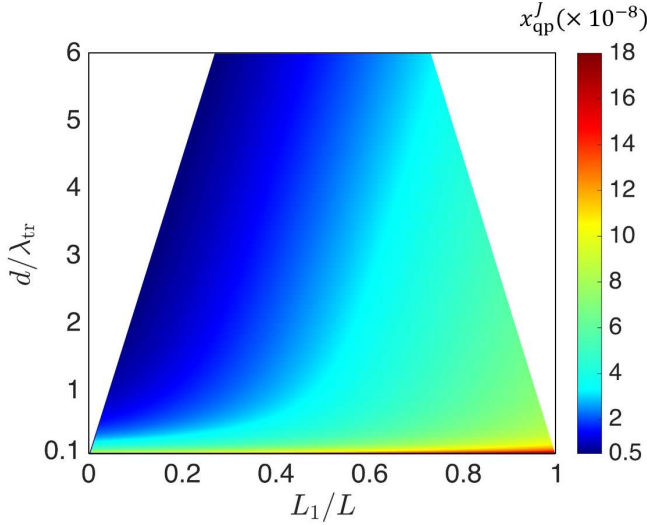
FIG. 5. Quasiparticle density at the junction as a function of trap location L_1 (in units of L) and its normalized size $d/\lambda_{\rm tr}$, calculated using $g = 10^{-4}\,\mathrm{Hz}$ [14, 25]; the normalization of the size d differs from that of Fig. 2, but the parameters used for the device are the same specified there.

For a long trap $d \gg \lambda_{\rm tr}$, we can still use Eq. (26) after the identification

$$\tau_w \to \frac{1}{\Gamma_{\rm eff}}\left(1 + \frac{A_L}{W\lambda_{\rm tr}}\right).\qquad(27)$$

With this substitution and for typical experimental parameters, we find again that the first term in Eq. (26) dominates when the trap is close to the junction (despite being smaller than the corresponding term for a short junction), while the second one takes over as L_1 increases. More generally, it should be noted that in any regime $x_{\rm qp}^J$ is a monotonically increasing function of L_1: as one could expect, the closer the trap is to the junction, the more it suppresses the quasiparticle density near the latter. This behavior is evident in Fig. 5: the plot clearly shows that the density is suppressed by placing the trap near to the gap capacitor, and that long traps $(d \gtrsim \lambda_{\rm tr})$ are more effective. Values as low as $x_{\rm qp} \sim 10^{-8}$ are predicted; for comparison, we note that in devices with the geometry considered here but without traps, we estimate $x_{\rm qp} \sim 10^{-6}$ [14]. On the other hand, for transmons with larger pads (so that there are always vortices that act as traps) we find $x_{\rm qp} \sim 10^{-7}$ [6, 14]. Further suppression of the density could be achieved by placing traps in the gap capacitor, since this would effectively reduce the uncovered area A_L [cf. Eq. (27)] between trap and junction.

Based on the above consideration, we do not expect that adding a second trap far from the junction significantly affects the steady-state density $x_{\rm qp}^J$ (we have confirmed this by direct calculation). Therefore, the results of the last two sections suggest that having two traps, one close to the junction and the other close to the pad

can both greatly reduce the steady-state density at the junction and enhance the decay rate of the excess density. Next, we show that traps can also contribute to the temporal stability of the qubit.

A. Fluctuations in the generation rate

As discussed previously, the density at the junction and hence the qubit relaxation rate are proportional to the generation rate g. Therefore, temporal variations in g can cause changes in the measured T_1 over time. Here we explore how traps can suppress these changes. For this purpose, we include Gaussian fluctuations of g in Eq. (1) by replacing $g \to g + \delta\widehat{g}(y, t)$, with

$$\langle \delta\widehat{g}(y, t)\rangle = 0,\qquad(28)$$

$$\langle \delta\widehat{g}(y, t)\,\delta\widehat{g}(y', t')\rangle = \gamma_g \delta(y - y')\frac{1}{2\tau_m}e^{-\frac{|t-t'|}{\tau_m}}.\qquad(29)$$

The parameter γ_g characterizes the fluctuation amplitude and has the same units as $\gamma_{\rm eff}$ of Eq. (7), while $\langle \ldots \rangle$ averages over all realizations of $\delta\widehat{g}$. We assume that fluctuations are spatially uncorrelated, but allow for temporal correlations with a finite memory time τ_m – we will return to this point in what follows. Note that under these assumptions the average density $\langle x_{\rm qp}(y)\rangle$ is in general a function of the spatial coordinate due to the presence of traps, but not of time.

To provide a measure for the density fluctuations at the junction position $y = 0$, we consider the quantity

$$\Delta x_{\rm qp}^2(t, t') \equiv \langle x_{\rm qp}(0, t)\,x_{\rm qp}(0, t')\rangle - \langle x_{\rm qp}(0)\rangle^2.\qquad(30)$$

This quantity can be expressed in terms of the eigenvalues $\mu_k < 0$ and eigenfunctions $n_k(y)$ of Eq. (1) (cf. Ref. [9] and Appendix B). Indeed, the quasiparticle density with the fluctuation term is

$$x_{\rm qp}(y, t) = -\sum_k \frac{1}{\mu_k}n_k(y)\,g_k$$
$$+ \sum_k \int_{-\infty}^t dt_1 e^{\mu_k(t-t_1)}n_k(y)\,\delta\widehat{g}_k(t_1),\qquad(31)$$

with

$$\delta\widehat{g}_k(t_1) = \int_0^L \frac{dy'}{L}n_k(y')\,\delta\widehat{g}(y', t_1),\qquad(32)$$

and the similar definition for g_k. Substituting this expression into the definition Eq. (30) and averaging over the fluctuations, we find

$$\Delta x_{\rm qp}^2(t, t') = \frac{\gamma_g}{2L}\frac{1}{\tau_m}\sum_k \int_{-\infty}^t dt_1 \int_{-\infty}^{t'} dt_2\, e^{\mu_k(t-t_1)}$$
$$\times e^{\mu_k(t'-t_2)}e^{-\frac{|t_1-t_2|}{\tau_m}}n_k^2(0).\qquad(33)$$

The time integrals are conveniently computed by first shifting the times t_1 and t_2 by t and t', respectively, and

then changing variables in the two-dimensional integral into a mean time $t_1 + t_2$ and time difference $t_1 - t_2$. After integration, we obtain

$$\Delta x_{\mathrm{qp}}^2 (t - t') = \frac{\gamma_g}{2L} \sum_k \frac{\tau_m e^{-\frac{|t-t'|}{\tau_m}} + \frac{1}{\mu_k} e^{\mu_k |t-t'|}}{\tau_m^2 \mu_k^2 - 1} n_k^2 (0) , \tag{34}$$

which depends only on time difference.

Equation (34) shows that even in the absence of time correlations for the fluctuations in the generation rate, $\tau_m = 0$, the fluctuation in the density are correlated due to diffusion. In this case, the longest decay time is that of the slowest mode, $1/\mu_0$, and is typically of the order of milliseconds [9]. This time is shorter than the time it takes to measure a qubit relaxation curve and hence estimate the quasiparticle density. Therefore, only the regime in which τ_m is much longer than $1/\mu_0$ could have observable consequences. Moreover, there is experimental evidence for slow fluctuations in the number of quasiparticles in qubits, obtained by monitoring the quantum jumps between states of a fluxonium, Ref. [25], and by repeated measurements, over several hours, of the relaxation time in a capacitively shunted flux qubit, Ref. [20]. Therefore, in the reminder of this section we focus only on the regime of long memory – that is, slow fluctuation in the generation rate. In the limit $\tau_m \gg 1/\mu_0$, Eq. (34) simplifies to

$$\Delta x_{\mathrm{qp}}^2 (t - t') \simeq \frac{\gamma_g}{2L\tau_m} e^{-\frac{|t-t'|}{\tau_m}} \sum_k \frac{1}{\mu_k^2} n_k^2 (0) . \tag{35}$$

We now want to establish that a trap can indeed reduce the fluctuations. To this end, we consider the simple case of the junction in a quasi-1D wire extending for length L from the junction and with a trap at distance L_1 from the junction. Initially, we take the trap to be small (length $d \ll \lambda_{\mathrm{tr}}$), and we distinguish between weak and strong trap, see Eq. (5). For a weak trap, $d \ll l_0$, the slow modes are only weakly dependent on the spatial coordinate. Moreover, for the slowest mode the decay rate is [cf. Eq. (3)]

$$\mu_0 \approx -\Gamma_{\mathrm{eff}} \frac{d}{L} , \tag{36}$$

while the higher modes are much faster, since $\mu_{n>0} \lesssim -D_{\mathrm{qp}}/L^2$, and thus $|\mu_{n>0}| \gg |\mu_0|$. Using $n_0(0) \approx 1$ and neglecting the small contributions from the higher modes, from Eq. (35) we find

$$\Delta x_{\mathrm{qp}}^2 (t - t') \approx \frac{\gamma_g}{2L\tau_m} e^{-\frac{|t-t'|}{\tau_m}} \left(\frac{L}{\Gamma_{\mathrm{eff}} d} \right)^2 . \tag{37}$$

This expression shows that a stronger/longer trap more effectively suppresses fluctuation, as could be expected.

In the case of a strong trap ($d \gg l_0$), the eigenmodes can be split in two sets (cf. Sec. III A): there are left and right modes, which are strongly suppressed to the

right and to the left of the trap, respectively (here we assume that the trap position is sufficiently far from the central position, see Appendix C). The left modes, with large amplitude between junction and trap, give small contributions to the density fluctuations when the trap is close to the junction and their contributions grow with junction-trap distance. The right modes, while being suppressed to the left of the trap, have opposite behavior with distance, so they can dominate when the trap is sufficiently close to the junction. Then we generically expect a non-monotonic dependence of the density fluctuations on trap-junction distance from the competition between modes to the left and right of the trap.

Let us consider the decay rates for left and right modes, which we denote with μ_{n,L_1} and $\mu_{n,L-L_1}$, respectively, where we define

$$\mu_{n,\ell} \simeq -D_{\mathrm{qp}} \left(\frac{\pi}{2\ell} \right)^2 (2n + 1)^2 , \ n = 0, 1, \ldots \tag{38}$$

Keeping in Eq. (35) only the slowest mode for each set, since the higher modes with $n > 0$ gives a smaller contribution to the sum, we find

$$\Delta x_{\mathrm{qp}}^2 (t - t') \approx \frac{\gamma_g}{L\tau_m} e^{-\frac{|t-t'|}{\tau_m}} \frac{1}{\mu_{0,L}^2}$$
$$\times \left[\left(\frac{L_1}{L} \right)^3 + \left(\frac{l_0}{d} \right)^2 \frac{L - L_1}{L} \right] , \tag{39}$$

where we used $n_{k,L_1}^2(0) \simeq 2L/L_1$ and $n_{k,L-L_1}^2(0) \simeq 2(l_0/d)^2 [L/(L-L_1)]^3$ (here we also assume $d \ll L_1, L - L_1$). The first term in square brackets originates from the lowest mode confined between junction and trap, while the second term, due to the lowest mode located on the other side of the trap, is suppressed by the small factor $(l_0/d)^2$. As a function of the trap position L_1, in agreement with the above considerations we find that Δx_{qp}^2 has a minimum at $L_1 = L l_0/d\sqrt{3}$, where the terms in square brackets take the approximate value $(l_0/d)^2$ and Eq. (39) takes the same form of Eq. (37). In fact, those terms rise significantly above this value only for $L_1 > L_f \equiv L(l_0/d)^{2/3}$, indicating that for a strong trap a large suppression of fluctuations can be achieved if the trap is not placed far beyond L_f. We note that this condition is more stringent than the one discussed after Eq. (26), $\tau_w = t_D$, which for the simple wire considered here gives a maximum distance $\sim 2L\sqrt{l_0/\pi d}$; in other words, maximum suppression of fluctuations ensures maximum suppression of the steady-state density.

The above considerations for a strong but short trap can be generalized to longer traps ($d \gtrsim \lambda_{\mathrm{tr}}$, with $d \ll L$) by substituting $l_0/d \to \lambda_{\mathrm{tr}}/L \sinh(d/\lambda_{\mathrm{tr}})$, see Appendix B. In both regimes (strong but short, and long trap), increasing the trap length suppresses the fluctuations at the junction, but shrinks the region over which maximum suppression can be achieved, since L_f becomes smaller. This region is however always small compared to the wire length, $L_f \ll L$. Together with the monotonic

dependence of the average quasiparticle density on distance obtained in the first part of this section, our results show that placing a trap close to the junction is effective in suppressing both the average density and its fluctuations, potentially making the qubit longer lived and more stable.

V. SUMMARY

In this paper we study the effects of size and position of normal-metal quasiparticle traps in superconducting qubits with large aspect ratio, so that quasiparticle diffusion can be considered one-dimensional. We focus on such a design because, as we argue at the end of Sec. II, in a two-dimensional setting traps must be large compared to the trapping length λ_{tr} [Eq. (6)] to be strong, while in quasi-1D it is sufficient for the trap length d to be longer than the characteristic scale l_0 [Eq. (5)] which accounts for diffusion, trapping rate, and device size – this characteristic scale is generally shorter than λ_{tr} for long devices ($L_{\mathrm{dev}} > \lambda_{\mathrm{tr}}$). A trap can influence the qubit in three ways: first, it suppresses the steady-state quasiparticle density at the junction; then the qubit's T_1 time can be increased, since this time is inversely proportional to the density. Second, a trap can speed up the decay of the excess quasiparticles and, third, it can decrease fluctuations around the steady-state density; these effects can render the qubit more stable in time – in fact, there is experimental evidence (Refs. [25] and [20]) that fluctuations in the number of quasiparticles are responsible for at least part of the temporal variations in T_1. Not surprisingly, a long trap ($d \gtrsim \lambda_{\mathrm{tr}}$) placed close to the junction is effective in all three aspects: fast decay of excess quasiparticles, suppression of the steady-state quasiparticle density (see Fig. 5), and suppression of density fluctuations at the junction. However, large traps could be a source of unwanted dissipation; therefore, we analyze in more detail the effects of shorter traps.

If a trap is weak, $d \lesssim l_0$, its position has little influence on the ability to suppress the quasiparticle density and its fluctuations, as well as on the decay rate of excess quasiparticles. Interestingly, for a strong but short trap, $l_0 \lesssim d \lesssim \lambda_{\mathrm{tr}}$, we find the position of the trap can be optimized in several ways. First, there is an optimal position that makes the decay of excess quasiparticles as fast as possible, see Figs. 2 and 3 in Sec. III A; however, a better choice is in general to divide a strong trap into smaller traps of length $\sim l_0$ and distribute those around the device, see Sec. III B. For the suppression of density fluctuations, we find that there is an optimal trap position, see Sec. IV A; more importantly, we find that there is a maximum distance L_f from the junction up to which the suppression of fluctuations is effective. Moreover, the distance up to which a large suppression of the steady-state density is achieved (Sec. IV) is longer than L_f, so that suppressing fluctuations also suppresses the steady-state density. Therefore, by correctly placing multiple

traps in the device in such a way that one is sufficiently close to the junction, all three beneficial effects of traps can be optimized.

The optimization of trap size, number, and placement is the only readily accessible way to improve the trap efficacy, since the effective trapping rate is limited by the energy relaxation rate in the normal metal [9], a material parameter that cannot be easily modified. We stress here that these considerations are valid for normal islands in tunnel contact with the superconductor – traps formed by gap engineering (e.g., by placing a lower-gap superconductor in good contact with the qubit) could behave differently and deserve further consideration.

Appendix A: Comparison with vortex trapping

In the coplanar gap capacitor transmon, the antenna pads are the widest part of the device. This makes it possible to trap vortices only in the pads when cooling the device in a small magnetic field. It was shown in Ref. [14] that each vortex added to a pad increases the density decay rate, and the effectiveness of trapping by vortices was characterized by a "trapping power" P. Here we compare the vortex trapping with a normal-metal trap covering the pad.

To determine the decay rate of the excess density x_{qp}, we construct the solution to the diffusion equation (1), along the lines of the Supplementary to Ref. [14]. We treat all parts of the device except the pad as one-dimensional and write x_{qp} in each segment in the form of Eq. (11). We approximate the density in the pad as uniform (justified for the lowest mode if $L_{\mathrm{pad}} < \lambda_{\mathrm{tr}}$, as in the actual devices). We then impose continuity of the density and current conservation where the parts of the device meet and thus arrive at the following effective boundary condition for the density at the connection between wire and pad (at $y = L$):

$$\frac{\partial x_{\mathrm{qp}}}{\partial y}\Big|_{y=L} = L_{\mathrm{pad}}^2 \left[\frac{D_{\mathrm{qp}}k^2 - \Gamma_{\mathrm{eff}}}{W D_{\mathrm{qp}}} \right] x_{\mathrm{qp}}(y = L) . \quad (A1)$$

Let us introduce for simplicity the dimensionless parameter $z = kL$; after imposition of all boundary conditions, as detailed in Ref. [14], we find that the parameter must satisfy the equation

$$\left(\frac{L_{\mathrm{pad}}^2 \Gamma_{\mathrm{eff}} t_L}{LW} \right) [1 - f(z)\tan z] - z[\tan z + f(z)] = 0 , \quad (A2)$$

with $t_L = L^2/D_{qp}$ and (see Ref. [14])

$$f(z) = \tan\left(z\frac{l}{L}\right) + 2\frac{W_c}{W}\tan\left(z\frac{L_c}{L}\right). \tag{A3}$$

The similar calculation for the case of $\bar{N}$ vortices in each pad leads to the following equation for z:

$$\left(\bar{N}\frac{Pt_L}{LW} - az^2\right)[1 - f(z)\tan z] - z[\tan z + f(z)] = 0 \tag{A4}$$

with $a = L_{pad}^2/(LW)$; since in the experiments a as well as z for the lowest mode and the coefficient multiplying $\bar{N}$ are all of order unity, in this equation we can neglect the term proportional to a for large number of vortices. Then, by comparing Eq. (A2) to Eq. (A4) we immediately see that for the vortex trapping to generate the same decay rate as the normal-metal trap, the number of vortices in each pad must be equal to:

$$\bar{N} = \frac{L_{pad}^2\Gamma_{eff}}{P}. \tag{A5}$$

Using $P = 6.7 \times 10^{-2}$ cm^2 s^{-1} and $L_{pad} = 80$ μm [14], the number of vortices in each pad would need to be $\bar{N} \simeq 230$. This shows that many vortices are needed to match the efficiency of the normal metal trap.

The cooling magnetic field needed to achieve this vortex number can be estimated to be $B \sim \bar{N}\Phi_0/S_{pad} \sim 0.75$ G, well into the regime in which the dissipation caused by the vortices negatively affect the qubit coherence [14]. A normal-metal island could also lead to dissipation. However, solving Eq. (A2) for the parameters specified in Fig. 2, we find a density decay rate $\tau_w^{-1} \approx 1.7$ms^{-1} for a metal-covered pad. From Fig. 2 we see that an optimally placed trap of length comparable to l_0 can achieve this decay rate, even though the trap area is much smaller than the pad area – thus, optimal placement can potentially limit the losses due to the normal metal. In contrast, allowing more vortices to enter the qubit (e.g., by fabricating wider wires or increasing the cooling magnetic field) is detrimental; indeed, in Ref. [14] at higher magnetic fields the qubit coherence time were found to shorten, likely due to vortices in the gap capacitor.

Appendix B: Finite-size trap

In this appendix, we treat a 1D system with a finite-size trap to identify the regime in which it can be considered as infinitely small. Moreover, we describe the crossover from infinitely small to finite size trap in the strong trapping regime.

We consider the 1D diffusion equation (where the spatial coordinate is $0 \leq y \leq L$)

$$\dot{x}_{qp} = D_{qp}\nabla^2 x_{qp} - \mathcal{A}(y)\Gamma_{eff}x_{qp}. \tag{B1}$$

We model the trap as a piece of length d, starting from $y = 0$, i.e., $\mathcal{A}(y) = 1$ for $y \leq d$ and 0 otherwise, see Fig. 6(a). Since no quasiparticle can leave the ends of the 1D wire, we adopt "hard wall" boundary conditions [28]

$$\left.\frac{\partial x_{qp}}{\partial y}\right|_{y=0} = \left.\frac{\partial x_{qp}}{\partial y}\right|_{y=L} = 0. \tag{B2}$$

The time-dependent solution of this problem can be expressed through the decomposition into eigenmodes, where

$$x_{qp}(y,t) = \sum_k e^{\mu_k t}\alpha_k n_k(y) \tag{B3}$$

and the eigenmodes fulfill

$$\mu_k n_k(y) = \left[D_{qp}\vec{\nabla}^2 - \mathcal{A}(y)\Gamma_{eff}\right]n_k(y). \tag{B4}$$

The eigenvalue problem can be solved with the Ansatz

$$n_k(y) = \frac{1}{\sqrt{N_k}}\begin{cases} \cos\left(\tilde{k}y\right), & y < d \\ a_k\cos(ky) + b_k\sin(ky), & y > d \end{cases} \tag{B5}$$

which satisfies the first boundary condition in Eq. (B2) and we defined

$$\tilde{k} = \sqrt{k^2 - \lambda_{tr}^{-2}}, \tag{B6}$$

with λ_{tr} of Eq. (6) and N_k is a normalization constant. From this Ansatz it follows that $\mu_k = -D_{qp}k^2$. Continuity of the function n_k and its derivative at $y = d$, together with the second condition in Eq. (B2), provide an equation for k:

$$k\tan[k(L-d)] = -\tilde{k}\tan\left(\tilde{k}d\right). \tag{B7}$$

While the modes thus defined provide the full time-evolution for all times, we are usually interested in the lowest mode which dominates the long-time behavior and which we denote with k_0. Assuming $k_0 \ll \lambda_{tr}^{-1}$, we have $\tilde{k}_0 \approx 1/\lambda_{tr}$ and we may approximate Eq. (B7) as

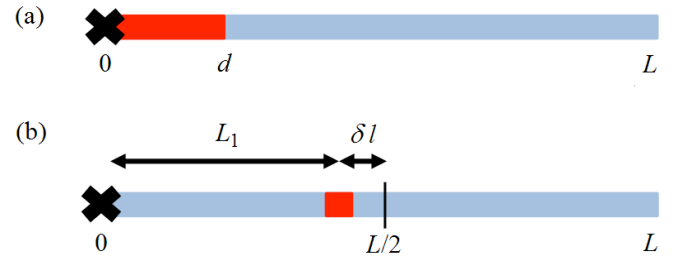$$l_{eff}k = \cot[k(L-d)], \tag{B8}$$

FIG. 6. Simplified systems considered in (a) Appendix B and (b) Appendix C. Blue/light grey denotes superconducting material and red/dark grey the part covered by the normal metal trap. The junction position marked with an X is at the origin of the wire of length L.

where we defined

$$l_{\text{eff}} = \lambda_{\text{tr}} \coth \left(\frac{d}{\lambda_{\text{tr}}} \right) . \qquad (B9)$$

In the case $d \ll \lambda_{\text{tr}}$ (which implies also $d \ll L$) Eq. (B8) becomes

$$\frac{\lambda_{\text{tr}}^2}{d} k = \cot(kL) , \qquad (B10)$$

which is equivalent to the model where the trap is represented by a delta function, $\mathcal{A}(y) \Gamma_{\text{eff}} \to \gamma_{\text{eff}} \delta(y)$, where $\gamma_{\text{eff}} = \Gamma_{\text{eff}} d$ and the trap is located at $y = 0$, see Ref. [9]. Here, in the strong trap limit, $d \gg l_0$ with l_0 of Eq. (5), we recover the diffusion-limited lowest mode

$$k_0 \approx \frac{\pi}{2L}. \qquad (B11)$$

This solution can be made more general using Eq. (B8). Namely, even when $d \gtrsim \lambda_{\text{tr}}$ (i.e., the trap is not small) we may identify the regime $l_{\text{eff}} \ll L - d$ in which

$$k_0 \approx \frac{\pi}{2} \frac{1}{L - d} . \qquad (B12)$$

This expression of course coincides with above diffusion-limited solution for $d \ll L$, and satisfies the initial assumption $k_0 \ll 1/\lambda_{\text{tr}}$ if $\lambda_{\text{tr}} \ll L - d$. Hence we may for instance increase d from $d \ll \lambda_{\text{tr}} \ll L$ to $\lambda_{\text{tr}} \ll d \ll L$, without changing the decay rate, as long as $l_{\text{eff}} \ll L$. However, the density of the mode close to the trap changes drastically with increasing d. Indeed, the normalization constant N_k in the limit $l_{\text{eff}}, d \ll L$ is given by

$$N_k \approx \frac{1}{2} \frac{1}{\lambda_{\text{tr}}^2 k^2} \sinh^2 \left(\frac{d}{\lambda_{\text{tr}}} \right) \qquad (B13)$$

and hence, the density at the origin for the lowest mode n_{k_0} becomes

$$n_{k_0}(0) \approx \frac{\pi}{\sqrt{2}} \frac{\lambda_{\text{tr}}}{L} \frac{1}{\sinh \left(\frac{d}{\lambda_{\text{tr}}} \right)} \qquad (B14)$$

which, for $d \ll \lambda_{\text{tr}}$ goes as

$$n_{k_0}(0) \sim \frac{l_0}{d} , \qquad (B15)$$

while for $d \gg \lambda_{\text{tr}}$ we find

$$n_{k_0}(0) \sim \frac{\lambda_{\text{tr}}}{L} e^{-\frac{d}{\lambda_{\text{tr}}}}. \qquad (B16)$$

As we see, by increasing d above the trapping length scale λ_{tr}, the density of quasiparticles gets exponentially suppressed near the trap. For a long trap $d \gg \lambda_{\text{tr}}$, such an exponential suppression takes place also for the steady-state density, as one can verify by reintroducing the generation rate g in the right hand side of Eq. (B1) and solving for the steady-state configuration with $\dot{x}_{\text{qp}} = 0$.

Appendix C: Quasi-degenerate modes and their observability

In this appendix, we consider the dependence of the lowest mode on the trap position. Moreover, we show that close to the optimal position the lowest and second lowest modes are quasi-degenerate. We finally comment on the consequences of this quasi-degeneracy on the observability of the lowest mode.

We take for simplicity a small trap ($d \ll \lambda_{\text{tr}}$) in a wire of length L, placed at an arbitrary distance L_1 from the origin, see Fig. 6(b); the quasiparticle density then obeys the diffusion equation (see [9] and App. B)

$$\dot{x}_{\text{qp}} = D_{\text{qp}} \nabla^2 x_{\text{qp}} - \delta(y - L_1) \gamma_{\text{eff}} x_{\text{qp}}. \qquad (C1)$$

To solve this equation, we look for eigenmodes n_k that must satisfy at $y = L_1$ the condition

$$l_{\text{sat}} \left[\partial_y n_k \left(L_1 + 0^+ \right) - \partial_y n_k^- \left(L_1 - 0^+ \right) \right] = n_k(L_1) \qquad (C2)$$

with $l_{\text{sat}} = \sqrt{D_{\text{qp}} t_{\text{sat}}}$, where $t_{\text{sat}} = D_{\text{qp}}/\gamma_{\text{eff}}^2$ (this condition follows from the standard procedure of integrating Eq. (C1) over an infinitesimal interval around L_1). The saturation time t_{sat} was introduced in Ref. [9] when studying the quasiparticle dynamics during injection and gives the time scale to reach a steady state. Here we use the related lengths scale l_{sat} to have a more compact notation: due to the identity

$$\frac{\pi}{2} \frac{l_{\text{sat}}}{L} = \frac{l_0}{d} , \qquad (C3)$$

this is not an independent parameter in the problem, and the strong (weak) trap condition can be expressed as $l_{\text{sat}} \ll L$ ($l_{\text{sat}} \gg L$).

As in the previous Appendix, see Eq. (B2), we assume "hard walls" on both ends, $\partial_y n_k(0) = \partial_y n_k(L) = 0$; then the eigenmodes are given by

$$n_k = \begin{cases} a_k \cos(ky) & \text{for } y < L_1 \\ b_k \cos[k(L-y)] & \text{for } y > L_1 \end{cases} . \qquad (C4)$$

These modes decay with a rate $1/\tau_k = D_{\text{qp}} k^2$. From Eq. (C2) and continuity of n_k, we find the condition for k

$$l_{\text{sat}} k \sin(kL) = \cos(kL_1) \cos[k(L - L_1)]. \qquad (C5)$$

For an infinitely strong trap, $l_{\text{sat}} \to 0$, we get the condition

$$\cos(kL_1) \cos[k(L - L_1)] = 0, \qquad (C6)$$

which provides for the lowest mode either $k = \frac{\pi}{2L_1}$ or $k = \frac{\pi}{2(L - L_1)}$ depending on whether $L - L_1 \gtrless L_1$. Note that the continuity of the modes at $y = l$ requires

$$a_k \cos(kL_1) = b_k \cos[k(L - L_1)] \qquad (C7)$$

which means that $b_k = 0$ for $k = \frac{\pi}{2L_1}$ or likewise $a_k = 0$ for $k = \frac{\pi}{2(L - L_1)}$. In other words, the trap effectively

separates the wire into two independent pieces, one to the left and one to right of the trap, with the quasiparticle density of the lowest mode fully suppressed in the shorter piece.

We define the optimal trap position as the one where the lowest mode decay rate is the highest. It is easy to see that this is at the degeneracy point, $L_1 = L/2$, where the two modes' decay rates coincide. Note however, that when passing the degeneracy point by increasing L_1 from $L_1 < L/2$ to $L_1 > L/2$, the eigenmode function jumps abruptly from being nonzero on the right hand side to nonzero on the left. Therefore, whether the quasiparticle density actually decays with the rate defined by the lowest mode, can be strongly affected by the initial conditions. In order to study this effect, we depart from the ideal, infinitely strong trap, and take a small but finite l_{sat}. In addition, we look at a system close to the degeneracy point, that is, $L_1 = L/2 + \delta l$ with $\delta l \ll L/2$. We first expand Eq. (C5) for small δl

$$l_{\text{sat}} k \sin(Lk) + \sin^2\left(\frac{Lk}{2}\right)(k\delta l)^2 = \cos^2\left(\frac{Lk}{2}\right). \quad \text{(C8)}$$

Next, we set $k = \pi/L + \delta k$ and, assuming a strong trap, $l_{\text{sat}} \ll L$, we expand up to second for $L\delta k \ll 1$ to find

$$4\pi^2 \frac{l_{\text{sat}}^2 + \delta l^2}{L^2} = \left(L\delta k + \frac{2\pi l_{\text{sat}}}{L}\right)^2. \quad \text{(C9)}$$

This results in

$$\delta k_{\mp} = 2\frac{\pi}{L}\left(-\frac{l_{\text{sat}}}{L} \mp \frac{\sqrt{l_{\text{sat}}^2 + \delta l^2}}{L}\right), \quad \text{(C10)}$$

and we see that the degeneracy at $\delta l = 0$ has been lifted by the small parameter l_{sat}/L.

From the continuity condition Eq. (C7), we are able to obtain for each mode the ratio between the (maximal) densities to the left and to the right of the trap

$$\frac{a_{k_{\mp}}}{b_{k_{\mp}}} = \frac{-\frac{\delta l}{L} - \frac{l_{\text{sat}}}{L} \mp \frac{\sqrt{l_{\text{sat}}^2 + \delta l^2}}{L}}{\frac{\delta l}{L} - \frac{l_{\text{sat}}}{L} \mp \frac{\sqrt{l_{\text{sat}}^2 + \delta l^2}}{L}}. \quad \text{(C11)}$$

In the limit $\delta l \ll l_{\text{sat}}$ this reduces to

$$\frac{a_{k_{\mp}}}{b_{k_{\mp}}} \simeq \pm 1. \quad \text{(C12)}$$

For $l_{\text{sat}} \ll \delta l$, on the other hand, we find

$$\frac{a_{k_{\mp}}}{b_{k_{\mp}}} \approx \pm\left(\frac{2|\delta l|}{l_{\text{sat}}}\right)^{\pm \text{sign}\delta l}, \quad \text{(C13)}$$

which is either very large or very small. This means that in this case the two modes have a very strong asymmetry in the relative density left and right of the trap.

This asymmetry can affect the measurement of the density decay rate, estimated via a local measurement

of the density in time. Let us suppose that we measure the quasiparticle density at $y = 0$. If $\delta l > 0$, the trap is further away from the detection point and thus the slower mode has a high density on the detector side; in this case we simply measure the slowest decay rate. On the contrary, if $\delta l < 0$ (with $|\delta l| \gg l_{\text{sat}}$), the faster mode has most of its density close to the origin and, depending on the time scale on which we measure, we may observe the higher decay rate. Let us suppose we have an initially homogeneous quasiparticle distribution, so that $b_{k_-} \approx a_{k_+}$. Due to the asymmetry of the two modes, the initial ($t = 0$) ratio r of the densities of the slowest to the faster mode at the origin $y = 0$ is

$$r(0) \equiv \frac{a_{k_-}}{a_{k_+}} \approx \frac{l_{\text{sat}}}{2|\delta l|} \ll 1. \quad \text{(C14)}$$

Hence initially, one can observe only the faster mode. As the decay progresses, this ratio eventually shifts in favor of the lowest mode,

$$r(t) = r(0)e^{-D_{\text{qp}}(k_-^2 - k_+^2)t} \approx \frac{l_{\text{sat}}}{2|\delta l|}e^{8\frac{|\delta l|}{L}\frac{t}{t_D}}, \quad \text{(C15)}$$

where we defined $t_D = \pi^2 D_{\text{qp}}/L^2$. The time at which the lowest mode becomes dominant can be estimated by setting $r(t) \sim 1$:

$$\frac{t}{t_D} \sim \frac{L}{8|\delta l|}\ln\frac{2|\delta l|}{l_{\text{sat}}}, \quad \text{(C16)}$$

where the right hand side is $\gg 1$. Thus, as we see, the time at which we can observe the decay of the lowest mode is much longer than t_D. This long time scale could also affect the choice of optimal trap placement, as we discuss in the next Appendix.

Appendix D: Effective length due to the pad

In the main text we discuss a device consisting of a long quasi-1D wire (length L and width W) with a square pad (side L_{pad}) at one end, see Fig 1. Here we show that for slow modes, the presence of the pad can be accounted for by the addition of an effective length to the original length of the wire. Indeed, let us assume that the decay times of the modes we are interested in are long compared to the diffusion time $\tau_{\text{pad}} = L_{\text{pad}}^2/D_{\text{qp}}$ across the pad. Then we can take the density in the pad to be approximately uniform, and this assumption leads to the following boundary condition [14]

$$\dot{x}_{\text{qp}}^{\text{wire}}(L) = -\frac{WD_{\text{qp}}}{L_{\text{pad}}^2}\partial_y x_{\text{qp}}^{\text{wire}}(L) \quad \text{(D1)}$$

for the density in the wire at the position where it joins the pad. We now show that this condition leads to a "hard wall" boundary condition for a 1D wire with an effective length which is longer due to the pad.

We use for $x_{\text{qp}}^{\text{wire}}$ an expansion analogous to Eq. (B3), where each mode in a 1D wire is generally of the form

$$n_k^{\text{wire}}(y) = a_k \cos(ky) + b_k \sin(ky). \qquad (D2)$$

Substituting such an expansion into Eq. (D1), and remembering that $\mu_k = -D_{\text{qp}}k^2$, we find

$$a_k\left[\widetilde{L}k\cos(Lk) + \sin(Lk)\right] = b_k\left[\cos(Lk) - \widetilde{L}k\sin(Lk)\right] \qquad (D3)$$

where we use the notation $\widetilde{L} = L_{\text{pad}}^2/W$. Defining the effective length addition for mode k as

$$L_{\text{pad}}^{\text{eff}}(k) = \frac{1}{k}\arcsin\left(\frac{\widetilde{L}k}{\sqrt{1+\widetilde{L}^2k^2}}\right) \qquad (D4)$$

we rewrite Eq. (D3) as

$$\tan\left[\left(L + L_{\text{pad}}^{\text{eff}}(k)\right)k\right] = \frac{b_k}{a_k}, \qquad (D5)$$

which indeed has the same form of the "hard wall" boundary condition for a wire of length $L + L_{\text{pad}}^{\text{eff}}$. For the limiting case $\widetilde{L}k \ll 1$, we find that $L_{\text{pad}}^{\text{eff}} \approx \widetilde{L}$ and hence, in this case, the effective total system length is $L + L_{\text{pad}}^2/W$.

Appendix E: Effective length due to the gap capacitor

Similarly to Appendix D, we show here that the gap capacitor provides an effective extension of the central wire. For this purpose, we add to one end of the wire of length L, two perpendicular wires, each of length L_c and width W_c, cf. Fig. 1 in the main text. Current conservation at the junction between the three wires provides the condition

$$W\left.\partial_y x_{\text{qp}}^{\text{wire}}\right|_{y=L} = -2W_c\left.\partial_x x_{\text{qp}}^c\right|_{x=L_c}. \qquad (E1)$$

Here, we assumed that the wire (gap capacitor) density is constant in the x- (y-) direction. The eigenmodes of wire and capacitor are of the form

$$n_k^{\text{wire}}(y) = a_k\cos(ky) + b_k\sin(ky),$$
$$n_k^c(x) = c_k\cos(kx).$$

Substituting this Ansatz into Eq. (E1) and requiring continuity at junction, we find the condition

$$a_k\left[\sin(Lk)\cos(L_ck) + 2\tfrac{W_c}{W}\sin(L_ck)\cos(Lk)\right]$$
$$= b_k\left[\cos(Lk)\cos(L_ck) - 2\tfrac{W_c}{W}\sin(L_ck)\sin(Lk)\right].$$

Defining the effective length addition due to the capacitor as

$$L_c^{\text{eff}}(k) = \frac{1}{k}\arcsin\left(\frac{2\frac{W_c}{W}\tan(L_ck)}{\sqrt{1+4\frac{W_c^2}{W^2}\tan^2(L_ck)}}\right), \qquad (E2)$$
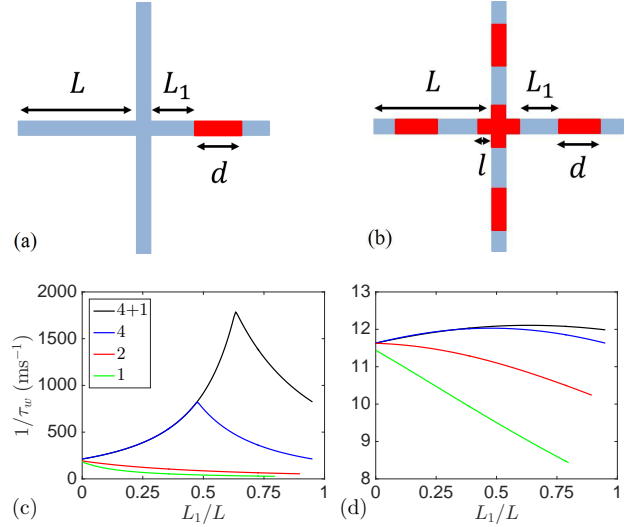

FIG. 7. (a) The single trap geometry. The trap is at distance L_1 from the center, and has size d. The 2 trap configuration follows from this setup, by adding a trap of the same size on the left branch, with the same distance L_1 from the center. (b) The $4+1$ trap geometry. All traps on the individual arms have the same distance L_1 from the center. The total trap size is $d' = 4l + 4d$. The 4-trap geometry follows from this one by removing the middle cross-like trap. (c) The resulting decay rate τ_w^{-1} as a function of L_1, for (bottom to top) 1, 2, 4, and $4+1$ traps. The parameters are $L = 150\,\mu$m and $\lambda_{\text{tr}} = 2\,\mu$m; the total trap length is 30 μm in all cases. (d) The decay rate as in (c), but with a realistic value $\lambda_{\text{tr}} = 86.3\,\mu$m for the trapping length.

we find the effective hard wall boundary condition

$$\frac{b_k}{a_k} = \tan\left[\left(L + L_c^{\text{eff}}(k)\right)k\right]. \qquad (E3)$$

Note that for $2W_c/W = 1$, the capacitor represents simply a direct extension to the wire with $L_c^{\text{eff}} = L_c$. For $L_ck \ll 1$ and $2W_c/W \ll 1/(L_ck)$, we may approximate $L_c^{\text{eff}} \approx 2\frac{W_c}{W}L_c$.

Appendix F: Traps in the Xmon geometry

In this Appendix we further explore the role of device geometry by studying the optimal placement of traps in the so-called Xmon qubit of Ref. [29]. We thus consider a four-arm geometry with symmetric arm lengths, see Fig. 7. Clearly, the optimal position for a single trap is at the center of the device; however, having two or three traps cannot lead to large improvement in the decay rate with respect to one trap, because the diffusion time cannot be shortened in all arms. Therefore, we need at least four traps, one in each arm, to improve τ_w^{-1}. A fifth should again be placed at the center, rather than in the arms. In fact, by generalizing the argument given at the beginning of Sec. III B, we find that the decay rate scales as $(N_{\text{tr}}/2)^2$ if N_{tr} is multiple of 4, and as $[(N_{\text{tr}}+1)/2]^2$ if

$N_{tr} = 4n+1$, $n = 0, 1, \ldots$ While in both cases the scaling is less favorable than the N_{tr}^2 one for a single wire, we see that for a small number of traps the configuration with the additional trap at the center gives a larger increase in the trapping rate.

To validate the above considerations, we solve the diffusion equation in the geometry obtained by simply joining four equally long 1D wires of length L. We consider 1, 2, 4 and 4+1 traps, all with the same total area, placed symmetrically as depicted in Fig. 7(a) and (b). We show the resulting decay rate τ_w^{-1} in Fig. 7(c) for a strong trap, obtained by assuming $\lambda_{\text{tr}} \ll L$. Comparing to the single-

trap case, we find the expected improvement by a factor of 4 (9) for 4 (4 + 1) traps. However, in an actual device the length is $L \approx 150\,\mu$m, which is not much larger than the estimate $\lambda_{\text{tr}} \approx 86.3\,\mu$m and gives, using Eq. (5), a trap size $l_0 \simeq 78\,\mu$m for the cross-over from weak to strong (diffusion-limited) trap. Therefore, in practice the traps are in the weak regime and their placement does not affect much the decay rate, see Fig. 7(d). This points to the need for stronger traps (with shorter λ_{tr}) for effective trapping in small devices. Alternatively, one could use traps in the ground plane surrounding the small device, to confine most quasiparticles away from it, see [30].

[1] R. Lutchyn, L. Glazman, and A. Larkin, Quasiparticle decay rate of Josephson charge qubit oscillations, Phys. Rev. B **72**, 014517 (2005).

[2] G. Catelani, J. Koch, L. Frunzio, R. J. Schoelkopf, M. H. Devoret, and L. I. Glazman, Quasiparticle Relaxation of Superconducting Qubits in the Presence of Flux, Phys. Rev. Lett. **106**, 077002 (2011).

[3] J. Leppäkangas and M. Marthaler, Fragility of flux qubits against quasiparticle tunneling, Phys. Rev. B **85**, 144503 (2012).

[4] M. D. Shaw, R. M. Lutchyn, P. Delsing, and P. M. Echternach, Kinetics of nonequilibrium quasiparticle tunneling in superconducting charge qubits, Phys. Rev. B **78**, 024503 (2008).

[5] J. M. Martinis, M. Ansmann, and J. Aumentado, Energy Decay in Superconducting Josephson-Junction Qubits from Nonequilibrium Quasiparticle Excitations, Phys. Rev. Lett. **103**, 097002 (2009).

[6] H. Paik, D. I. Schuster, L. S. Bishop, G. Kirchmair, G. Catelani, A. P. Sears, B. R. Johnson, M. J. Reagor, L. Frunzio, L. I. Glazman, S. M. Girvin, M. H. Devoret, and R. J. Schoelkopf, Observation of High Coherence in Josephson Junction Qubits Measured in a Three-Dimensional Circuit QED Architecture, Phys. Rev. Lett. **107**, 240501 (2011).

[7] D. Ristè, C. C. Bultink, M. J. Tiggelman, R. N. Schouten, K. W. Lehnert, and L. DiCarlo, Millisecond charge-parity fluctuations and induced decoherence in a superconducting transmon qubit, Nat. Commun. **4**, 1913 (2013).

[8] I. M. Pop, K. Geerlings, G. Catelani, R. J. Schoelkopf, L. I. Glazman, and M. H. Devoret, Coherent suppression of electromagnetic dissipation due to superconducting quasiparticles, Nature **508**, 369 (2014).

[9] R.-P. Riwar, A. Hosseinkhani, L. D. Burkhart, Y. Y. Gao, R. J. Schoelkopf, L. I. Glazman, G. Catelani, Normal-metal quasiparticle traps for superconducting qubits, Phys. Rev. B **94**, 104516 (2016).

[10] J. Aumentado, M. W. Keller, J. M. Martinis, and M. H. Devoret, Nonequilibrium Quasiparticles and 2e Periodicity in Single-Cooper-Pair Transistors, Phys. Rev. Lett. **92**, 066802 (2004).

[11] L. Sun, L. DiCarlo, M. D. Reed, G. Catelani, L. S. Bishop, D. I. Schuster, B. R. Johnson, Ge A. Yang, L. Frunzio, L. Glazman, M. H. Devoret, and R. J. Schoelkopf, Measurements of Quasiparticle Tunneling Dynamics in a Band-Gap-Engineered Transmon Qubit, Phys. Rev. Lett. **108**, 230509 (2012).

[12] J. N. Ullom, P. A. Fisher and M. Nahum, Magnetic field dependence of quasiparticle losses in a superconductor, Appl. Phys. Lett. **73**, 2494 (1998).

[13] I. Nsanzineza and B. L. T. Plourde, Trapping a Single Vortex and Reducing Quasiparticles in a Superconducting Resonator, Phys. Rev. Lett. **113**, 117002 (2014).

[14] C. Wang, Y. Y. Gao, I. M. Pop, U. Vool, C. Axline, T. Brecht, R. W. Heeres, L. Frunzio, M. H. Devoret, G. Catelani, L. I. Glazman, and R. J. Schoelkopf, Measurement and control of quasiparticle dynamics in a superconducting qubit, Nat. Commun. **5**, 5836 (2014).

[15] M. Taupin, I. M. Khaymovich, M. Meschke, A. S. Melnikov, and J. P. Pekola, Tunable quasiparticle trapping in Meissner and vortex states of mesoscopic superconductors, Nat. Commun. **7**, 10977 (2016).

[16] N. A. Court, A. J. Ferguson, Roman Lutchyn, and R. G. Clark, Quantitative study of quasiparticle traps using the single-Cooper-pair transistor, Phys. Rev. B **77**, 100501(R) (2008).

[17] S. Rajauria, H. Courtois, and B. Pannetier, Quasiparticle-diffusion-based heating in superconductor tunneling microcoolers, Phys. Rev. B **80**, 214521 (2009).

[18] S. Rajauria, L. M. A. Pascal, Ph. Gandit, F. W. J. Hekking, B. Pannetier, and H. Courtois, Efficiency of quasiparticle evacuation in superconducting devices, Phys. Rev. B **85**, 020505(R) (2012).

[19] O.-P. Saira, A. Kemppinen, V. F. Maisi, and J. P. Pekola, Vanishing quasiparticle density in a hybrid Al/Cu/Al single-electron transistor, Phys. Rev. B **85**, 012504 (2012).

[20] S. Gustavsson, F. Yan, G. Catelani, J. Bylander, A. Kamal, J. Birenbaum, D. Hover, D. Rosenberg, G. Samach, A. P. Sears, S. J. Weber, J. L. Yoder, J. Clarke, A. J. Kerman, F. Yoshihara, Y. Nakamura, T. P. Orlando, W. D. Oliver, Suppressing relaxation in superconducting qubits by quasiparticle pumping, Science **354**, 1573 (2016).

[21] A. Zazunov, V. S. Shumeiko, E. N. Bratus, J. Lantz, and G. Wendin, Andreev Level Qubit, Phys. Rev. Lett. **90**, 087003 (2003).

[22] C. Janvier, L. Tosi, L. Bretheau, Ç. Ö. Girit, M. Stern, P. Bertet, P. Joyez, D. Vion, D. Esteve, M. F. Goffman, H. Pothier, C. Urbina, Coherent manipulation of Andreev states in superconducting atomic contacts, Science **349**, 1199 (2015).

[23] D. Rainis and D. Loss, Majorana qubit

decoherence by quasiparticle poisoning, Phys. Rev. B **85**, 174533 (2012).

[24] J. P. Pekola, O.-P. Saira, V. F. Maisi, A. Kemppinen, M. Möttönen, Y. A. Pashkin, and D. V. Averin, Single-electron current sources: Toward a refined definition of the ampere, Rev. Mod. Phys. **85**, 1421 (2013).

[25] U. Vool, I. M. Pop, K. Sliwa, B. Abdo, C. Wang, T. Brecht, Y. Y. Gao, S. Shankar, M. Hatridge, G. Catelani, M. Mirrahimi, L. Frunzio, R. J. Schoelkopf, L. I. Glazman, and M. H. Devoret, Non-Poissonian Quantum Jumps of a Fluxonium Qubit due to Quasiparticle Excitations, Phys. Rev. Lett. **113**, 247001 (2014).

[26] When calculating decay rates, a finite s_b can be simply added to those obtained for $s_b = 0$; for typical parameters, this addition is small. Equivalently, we note that the length scale $\sqrt{D_{qp}/s_b}$ is much longer than all other length scales in the problem, which justifies neglecting s_b. We also neglect recombination, see Ref. [9].

[27] R.-P. Riwar, L. I. Glazman, and G. Catelani (unpublished).

[28] The validity of the boundary condition at $y = 0$ can be justified by imagining a short piece of uncovered superconductor extending to the left of the trap, $-\epsilon < y < 0$. Then clearly we have $\partial x_{qp}/\partial y|_{y=-\epsilon} = 0$; taking the limit $\epsilon \to 0$ and since x_{qp} and its derivative are continuous, we arrive at Eq. (B2). A particular case is that of a point-like trap with $d \to 0$ and a finite, fixed value of $\gamma_{eff} = d\Gamma_{eff}$; then one can either follow the procedure just described, or equivalently, use the boundary condition $\partial x_{qp}/\partial y|_{y=0} = x_{qp}(0)\gamma_{eff}/D_{qp}$, see Eq. (C2).

[29] R. Barends, J. Kelly, A. Megrant, D. Sank, E. Jeffrey, Y. Chen, Y. Yin, B. Chiaro, J. Mutus, C. Neill, P. O'Malley, P. Roushan, J. Wenner, T. C. White, A. N. Cleland, and J. M. Martinis, Coherent Josephson Qubit Suitable for Scalable Quantum Integrated Circuits, Phys. Rev. Lett. **111**, 080502 (2013).

[30] U. Patel, I. V. Pechenezhskiy, B. L. T. Plourde, M. G. Vavilov, and R. McDermott, Phonon-Mediated Quasiparticle Poisoning of Superconducting Microwave Resonators, arXiv:1610.09351.